Redox Biology 60 (2023) 102625

Contents lists available at ScienceDirect

Redox Biology

journal homepage: www.elsevier.com/locate/redox

Hydropersulfides (RSSH) attenuate doxorubicin-induced cardiotoxicity while boosting its anticancer action

Blaze M. Pharoah [a,1], Chengximeng Zhang [a,1], Vinayak S. Khodade [a], Gizem Keceli [b], Christopher McGinity [d], Nazareno Paolocci [b,c,**], John P. Toscano [a,*]

[a] Department of Chemistry, Johns Hopkins University, Baltimore, MD 21218, United States
[b] Division of Cardiology, Johns Hopkins University School of Medicine, Baltimore, MD 21205, United States
[c] Department of Biomedical Sciences, University of Padova, Padova, Italy
[d] Center for Cancer Research, National Cancer Institute, Frederick, MD 21702, United States

ARTICLE INFO

Keywords:
Hydropersulfides
Doxorubicin-induced cardiotoxicity
Cytoprotection
Nrf2
PGC-1α
Reductive stress

ABSTRACT

Cardiotoxicity is a frequent and often lethal complication of doxorubicin (DOX)-based chemotherapy. Here, we report that hydropersulfides (RSSH) are the most effective reactive sulfur species in conferring protection against DOX-induced toxicity in H9c2 cardiac cells. Mechanistically, RSSH supplementation alleviates the DOX-evoked surge in reactive oxygen species (ROS), activating nuclear factor erythroid 2-related factor 2 (Nrf2)-dependent pathways, thus boosting endogenous antioxidant defenses. Simultaneously, RSSH turns on peroxisome proliferator-activated receptor gamma coactivator 1-alpha (PGC-1α), a master regulator of mitochondrial function, while decreasing caspase-3 activity to inhibit apoptosis. Of note, we find that RSSH potentiate anticancer DOX effects in three different cancer cell lines, with evidence that suggests this occurs via induction of reductive stress. Indeed, cancer cells already exhibit much higher basal hydrogen sulfide (H_2S), sulfane sulfur, and reducing equivalents compared to cardiac cells. Thus, RSSH may represent a new promising avenue to fend off DOX-induced cardiotoxicity while boosting its anticancer effects.

1. Introduction

Mortality rates associated with cancer are decreasing [1], owing to advancements in cytotoxic chemotherapy that remains a therapeutic pillar for many forms of cancer. Anthracyclines, such as doxorubicin (DOX), are well-established and highly effective antineoplastic agents used to treat several adult and pediatric cancers, such as breast cancer, leukemia, lymphomas, sarcomas, and many others [2]. However, this success comes with the unfortunate cost of a heightened risk of developing cardiotoxicity [3,4], a clinical condition that has thus far evaded an effective treatment.

DOX-induced cardiotoxicity (DIC), in particular, can occur either acutely or more chronically [5]. Distinctive DIC pathological features include increased reactive oxygen species (ROS) production [6], defects in iron handling [7,8], and inhibition of topoisomerase 2β (Top2β) [9], which is heavily expressed in cardiomyocytes. Thus, the pathogenesis of DIC is multifactorial. As a consequence, therapies targeting just one of these stigmata are unlikely to afford sizable, clinically-relevant protection against DIC. From a pathobiological point of view, cardiomyocytes are exquisitely vulnerable to ROS-mediated cellular damage due to their lower constitutive levels of antioxidant enzymes [10,11]. Furthermore, DOX tends to accumulate in mitochondria, thus perturbing cardiac cell bioenergetics and function [12]. Of note, mitochondria retain the memory of redox and metabolic challenges beyond the DOX *in vivo* half-life [13]; this phenomenon, in turn, renders cancer patients more sensitive to cumulative regimens of drug therapy. Against this background, an ideal anti-DIC drug should target more than one facet of the DIC pathology.

Antioxidants such as ascorbic acid, *N*-acetylcysteine (NAC), carvedilol, and coenzyme Q10, although promising at the preclinical stage, have met with limited success clinically against DIC [14]. This failure could be due to their inability to reach the ROS sources in efficacious amounts; another explanation is that the enhanced ROS emission could be the epiphenomenon of substantial structural/functional alterations in

* Corresponding author.
** Corresponding author. Division of Cardiology, Johns Hopkins University School of Medicine, Baltimore, MD 21205, United States.
E-mail addresses: npaoloc1@jhmi.edu (N. Paolocci), jtoscano@jhu.edu (J.P. Toscano).
[1] These authors equally contributed to this work.

https://doi.org/10.1016/j.redox.2023.102625
Received 12 December 2022; Received in revised form 19 January 2023; Accepted 1 February 2023
Available online 4 February 2023

mitochondria, and potentially elsewhere. Currently, the only FDA-approved anti-DIC drug is dexrazoxane (DRZ) [15], an iron chelator that inhibits lipid peroxidation and cellular damage [16]. Yet, despite its effectiveness, DRZ is not devoid of side effects, such as hematological toxicity, altered liver function, and pain [17,18]. In essence, no current optimal strategy for preventing and/or managing DIC remains a significant unmet clinical milestone. Another unique challenge in cardio-oncology is to develop a therapeutic agent that selectively protects the heart against anticancer agents such as DOX without jeopardizing its therapeutic effectiveness. However, tackling this issue must stem from a deeper understanding of the different response of myocardial cells vs. cancer cells towards diverse potential stressors, such as ROS.

Hydrogen sulfide (H_2S) and related reactive sulfur species (RSS) have emerged as critical signaling molecules in the cardiovascular system. Their systemic administration results in significant protection against many cardiovascular disorders, including ischemia-reperfusion injury [19–22]. Moreover, H_2S can attenuate DOX-mediated toxic effects in H9c2 cells [23–26], with mechanisms, however, that remain to be fully understood. Post-translational modification of redox-active cysteines (Cys-SH) into cysteine hydropersulfides (Cys-SSH) is now recognized as a critical step in H_2S signaling [27–29]. Sulfane sulfur species like hydropersulfides (RSSH) and polysulfides can readily modify protein cysteine residues (P-SH), generating protein hydropersulfides (P-SSH) [30,31]. Accordingly, H_2S biological effects are now ascribed substantially to RSSH [32,33] and not entirely to H_2S *per se*. Cys-SSH and glutathione hydropersulfide (GSSH) are prevalent in mammalian tissues and fluids [34,35]. Intriguingly, RSSH exhibit potent cytoprotective effects against oxidative and/or electrophilic stress [36,37]. Indeed, we recently demonstrated that exogenous RSSH administration at reperfusion outweighs other H_2S-related species or classical post-conditioning in limiting post-ischemic cardiac injury, i.e., infarct size and dysfunction [38].

Inspired by these findings, we designed the present study to address the following specific questions: 1) Does RSSH effectively protect cardiomyocytes against DIC? 2) Does it do so without compromising the anticancer action of DOX? 3) Do the differing effects in cancer vs. cardiac cells depend, at least partly, on a substantially different redox milieu in each cell type? Answering the latter question, in particular, would not only provide a mechanism explaining RSSH beneficial actions against DIC, but also fill a gap in our current knowledge of the different pathobiology of cardiac vs. cancer cells.

2. Materials and methods

2.1. Reagents

Sodium sulfide (Na_2S) was purchased from TCI chemicals. *N*-acetyl cysteine was purchased from Sigma Aldrich. Dexrazoxane was obtained from Cayman Chemical. Doxorubicin was purchased from Astatech Inc. H_2S donor **1** [39], RSSH donor **AST** [40], and *N*-acetyl-*O*-ethyl cysteine trisulfide (Cys-S_3) [38] were synthesized following reported procedures. Na_2S (10 mM) and Na_2S_3 (10 mM) stock solutions were freshly prepared in molecular biology-grade water (Corning). The stock solutions of **AST** and Cys-S_3 were prepared in DMSO:Water (<0.001%) and diluted fresh each day before administration.

2.2. Cell culture

H9c2 embryonic rat heart myoblasts were obtained from the American Type Culture Collection and were cultured at 37 °C in Dulbecco's modified Eagle's medium (Gibco) supplemented with 10% fetal bovine serum (FBS,ThermoFisher) in an atmosphere with 5% CO_2. They were propagated in T75-flasks, split before reaching 70–80% confluence (usually every day or every second day), and used within 11 passages. MDA-MB-468, MCF-7 and HepG2 cells were also obtained from the American Type Culture Collection. These cells were cultured in RPMI 1640 media (Gibco) supplemented with 10% fetal bovine serum (FBS, ThermoFisher), penicillin, and streptomycin (50 U/mL) (Life Technologies, Inc.) at 37 °C in an atmosphere with 5% CO_2. Cells were trypsinized before seeding with the desired density.

2.3. Cell viability assays

(a) Cell viability using CCK-8 assay

Viability and cytotoxicity were tested using the Cell Counting Kit-8 (Dojindo, CK-04) [41]. H9c2, MDA-MB-468, MCF-7, and HepG2 cells were independenlty seeded with a density of 15,000 cells per well into 96-well plates. The plates were incubated at 37 °C for 24 h before treatment. The cells were first treated with **AST** ranging from 6.3 μM to 200 μM for 4 h. After 4 h pretreatment, the media was replaced with **AST** and with or without 5 μM of DOX for another 24 h. After the 24 h treatment, the media was replaced with SANS media (190 μL/well) and CCK-8 solution (10 μL/well), followed by incubation for 1–2.5 h (2.5 h for H9c2 cells, 2 h for MDA-MB-468 and MCF-7 cells, and 1 h for HepG2 cells). Colorimetric measurements were conducted at 450 nm absorbance using a SpectraMax microplate reader (Molecular Devices). Each treatment group was normalized to the vehicle loaded control group.

(b) Cell viability using Sytox Green stain

H9c2 cells were seeded at a density of 1.5×10^4 cells/well. After 24 h, the media was replaced, and **AST** added via 20 μL volumes using DMSO:H_2O (<0.01% DMSO) as the vehicle. Cells were incubated for an additional 24 h before the media was removed. Then, 100 μL of media containing 3 μM Sytox Green nucleic acid stain (Invitrogen) was added and the cells were incubated for 2 h before fluorescence readings were obtained at $485_{Ex}/538_{Em}$ (Step 1). Finally, an additional 100 μL of media containing 3 μM Sytox and 0.2% Triton X-100 was added to permeabilize all cells and incubated for 1 h before fluorescence values were again measured (Step 2). The relative percent of cells surviving was calculated as 100% minus the ratio of the fluorescence value of Step 1 over Step 2 (% cells surviving = 100% - (FL_{538} (Step 1)/FL_{538}(Step 2)).

2.4. Measurement of reactive oxygen species (ROS) by electronic paramagnetic resonance (EPR) spectroscopy

H9c2 and MDA-MB-468 cells with a density of 1×10^6 were plated into 100 mm × 20 mm tissue culture plates and incubated at 37 °C for 24 h before treatment. The cells were treated with 0 or 25 μM **AST** for 4 h followed by co-treatment with 5 μM DOX or vehicle for another 4 h. After the incubation, the cells were washed with phosphate-buffered saline (PBS) twice and scraped into 250 μL of pH 7.4 PBS containing 0.1 mM diethylenetriaminepentaacetic acid (DTPA) and protease inhibitor cocktail (Roche Applied Science, Indianapolis, IN). ROS measurements were conducted as previously described [42,43]. Briefly, stock solutions of 1-hydroxy-3-methoxycarbonyl-2,2,5,5-tetramethylpyrrolidine hydrochloride (CMH; Enzo Life Sciences, Farmingdale, NY) and 1-hydroxy-4-[2-triphenylphosphonio)-acetamido]-2,2,6,6-tetramethylpiperidine (mitoTEMPO-H; Enzo Life Sciences, Farmingdale, NY) were prepared daily in nitrogen-purged 0.9% (w/v) NaCl, 25 g/L Chelex 100 (Bio-Rad) and 0.1 mM DTPA, and kept on ice [44]. For detection of global ROS levels, the samples were treated with 1 mM CMH at RT for 10 min, transferred to 0.05 mL glass capillary tubes, and analyzed on a Bruker E-Scan (Billerica, MA) electron paramagnetic resonance (EPR) spectrometer. To determine mitochondrial ROS levels, the samples were incubated with the mitochondria-specific spin probe, mitoTEMPO-H (160 μM), at 37 °C for 15 min and analyzed as described above. Spectrometer settings were as follows: sweep width, 100 G; microwave frequency, 9.75 GHz; modulation amplitude, 1 G; conversion time, 5.12 ms; receiver gain, 2×10^3; the number of scans, 16 (global

ROS levels) or 256 (mitochondrial ROS levels). EPR signal intensities were normalized to the protein concentrations of the cell lysates determined by Pierce BCA protein assay kit (Life Technologies).

2.5. Caspase-3-like activity

H9c2 cells were seeded at a density of 1×10^6 cells/dish and incubated in a humidified atmosphere containing 5% CO_2 at 37 °C for 24 h. After incubation, cells were treated with 0 or 25 μM **AST** for 4 h followed by the addition of 5 μM DOX for an additional 4 h. After incubation, cells were washed 3 times with PBS (pH 7.4) before collection in PBS and further processing according to the manufacturer's instruction (ab39401) [45].

2.6. Cytosolic and Nuclear Extraction

MDA-MB-468 cells were plated with a density of 1.0×10^6 into 100 mm × 20 mm tissue culture plates (Corning) in RPMI (Gibco) with 10% FBS (ThermoFisher) and incubated at 37 °C in a humidified atmosphere containing 5% CO_2 for 72 h H9c2 cells with density of 1.0×10^6 cells per plate were plated into 150 mm × 20 mm tissue culture plates (Falcon) in DMEM (Gibco) with 10% FBS (ThermoFisher) and incubated at 37 °C in a humidified atmosphere containing 5% CO_2 for one week. After incubation, the cells were treated with 0, 25, and 50 μM **AST** for 24 h followed by co-treatment of 0, 25, and 50 μM of **AST** with or without 0.5 μM DOX for another 24 h. After incubation, the cells were trypsinized and centrifuged at 1000×*g* for 5 min. The cells were then washed with 1.5 mL of cold PBS and collected at 2000×*g* for 5 min. The cell pellets were lysed and fractionalized with Nuclear/Cytosol Fractionation Kit (Biovision, K266) according to the manufacturer's protocols (100 μl cytosolic extraction buffer and 50 μl Nuclear Extraction buffer). The cytosolic and nuclear lysate were stored at −80 °C before immunoblotting.

2.7. Electrophoresis and Western blot

Cells were lysed in RIPA (Thermo Scientific) with Protease inhibitor (1:100) and protein concentrations were determined by Pierce BCA protein assay kit (Life Technologies). All gels and Western blots were run using a Bio-Rad Mini-Protean II electrophoresis and Western blotting system. Samples were prepared in SDS Laemmli buffer and dithiothreitol (DTT, 50 mM). SDS-PAGE using 4–20% polyacrylamide was performed following standard protocols [46]. Upon separation by gel electrophoresis, the proteins were transferred via Western blotting onto nitrocellulose membranes. The proteins were detected using rabbit polyclonal antibody, anti-PGC-1α (1:1000 dilution, Novus biologicals, NBP1-04676), rabbit monoclonal antibodies, anti-GAPDH (1:1000 dilution, Cell Signaling, 2118), anti-Lamin A/C (1:1000 dilution, Cell Signaling, 2032), mouse monoclonal antibodies anti-Nrf2 (1:1000 dilution, Santa Cruz, sc-365949), anti-NQO1 (1:500 dilution, Cell Signaling, 3187), anti-mtTFAM (1:1000 dilution, Santa Cruz, sc-166965) and anti-Lamin A/C (1:1000 dilution, Cell Signaling, 4777). Primary antibody binding was visualized by using the secondary antibodies IRDye 680LT goat anti-rabbit IgG (1:10000 dilution, Li-Cor Biosciences, 926–68021) and IRDye 800CW goat anti-mouse IgG (1:10000 dilution, Li-Cor Biosciences, 926–32210). Since the molecular weights of the proteins of interest are distinct, we used the same membrane to detect different proteins. The membrane was incubated with one primary antibody at a time followed by incubation with the secondary antibody. The sequence of protein detection was – (1) NQO1, (2) Nrf2, (3) TFAM, (4) PGC-1α, (5) loading control Lamin A, and (6) loading control GAPDH. Membranes were scanned on an Odyssey scanner (Li-Cor Biosciences), and the bands were quantified using Empiria Studio software (version 2.1.1.138).

2.8. Sulfane sulfur and H_2S detection assay

Sulfane sulfur and H_2S levels were detected by the respective fluorescence probe of Sulfobiotics SSP4 [47] (Dojindo, SB10) and Sulfobiotics Hsip-1 DA [48] (Dojindo, SB22). Cells were seeded at a density of 500,000 cells/well in a 6-well plate in 2 mL media and incubated at 37 °C for 24 h. After 24 h, 2 mL fresh media with or without 1 μM DOX was added and incubated at 37 °C for 24 h. After treatment, media was changed (1 mL total) conatining SSP4 (20 μM) or Hsip-1 (5 μM) and cetyltrimethylammonium bromide (CTAB) (100 μM) and incubated for 30 min. After treatment with SSP4 and Hsip-1 probes, cells were washed 3 times with warm PBS and finally resuspended in 1 mL PBS. Fluorescence measurement were performed at $\lambda_{ex} = 491$ nm, $\lambda_{em} = 516$ nm for HSip-1 and $\lambda_{ex} = 482$ nm, $\lambda_{em} = 515$ nm for SSP4 with SpectraMax microplate reader (Molecular Devices). After measurement, PBS was removed, the cells were trypsinized and collected for counting.

2.9. $NADH/NAD^+$ assay

H9c2, MDA-MB-468, MCF-7 and HepG2 cells (1.0×10^6 cells per plate) were plated into 100 mm × 20 mm tissue culture plates (Corning) in respective media supplemented with 10% FBS (ThermoFisher) and incubated at 37 °C in a humidified atmosphere containing 5% CO_2 for 48 h. After incubation, the cells were scraped with cold PBS and centrifuged at 1000×*g* for 5 min. The cells were further washed with 1.5 mL cold PBS and collected after centrifugation at 2000×*g* for 5 min. The cell pellets were lysed using buffer supplied with commercial assay kits following the manufacturer's instructions (Abcam ab65348). Each sample were deproteinized with 10 kDa spin column (ThermoFisher, PI88513) and centrifuged at 15000×*g* for 10 min. The supernatant containing metabolites were saved and colorimetric measurements were made at 450 nm absorbance with SpectraMax microplate reader (Molecular Devices). NADH and NAD + concentrations were determined from standard calibration curve according to the manufacturer's instructions [49].

2.10. GSH/GSSG assay

H9c2, MDA-MB-468, MCF-7, and HepG2 cells with a density of 1.0×10^6 cells per plate were plated into 100 mm × 20 mm tissue culture plates (Corning) in DMEM (Gibco, H9c2) and RPMI (Gibco, MDA-MB-468, MCF-7 and HepG2) with 10% FBS (ThermoFisher) and incubated at 37 °C in a humidified atmosphere containing 5% CO2 for 72 h H9c2, MDA-MB-468 were treated with 0, 25, and 50 μM **AST** for 24 h followed by co-treatment of 0, 25, and 50 μM **AST** with or without 0.5 μM DOX for another 24 h. After incubation, the cells were trypsinized and centrifuged at 1000×*g* for 5 min. The cells were then washed with 1.5 mL of cold PBS and collected after centrifugation at 2000×*g* for 5 min. The cell pellets were lysed with buffer supplied with commercial assay kits following the manufacturer's instructions (Abcam ab239709). Colorimetric measurements were made at 405 nm absorbance with SpectraMax microplate reader (Molecular Devices). GSH and toal glutathione concentrations were determined from respective standard calibration curves according to the manufacturer's instructions. The GSSG concentration were calculated by subtracting GSH from total glutathione [50].

2.11. Data analysis

Data were analyzed and graphs were created using GraphPad Prism software (version 9.3.1). Data are presented as mean ± standard error of the mean. Statistical analyses were performed by using one-way or two-way ANOVA followed by post-hoc multiple comparison test for data involving more than two groups. If testing suggested the data were not normally distributed (Shapiro-Wilk test for normality), comparisons performed with the non-parametric Kruskal-Wallis test followed by

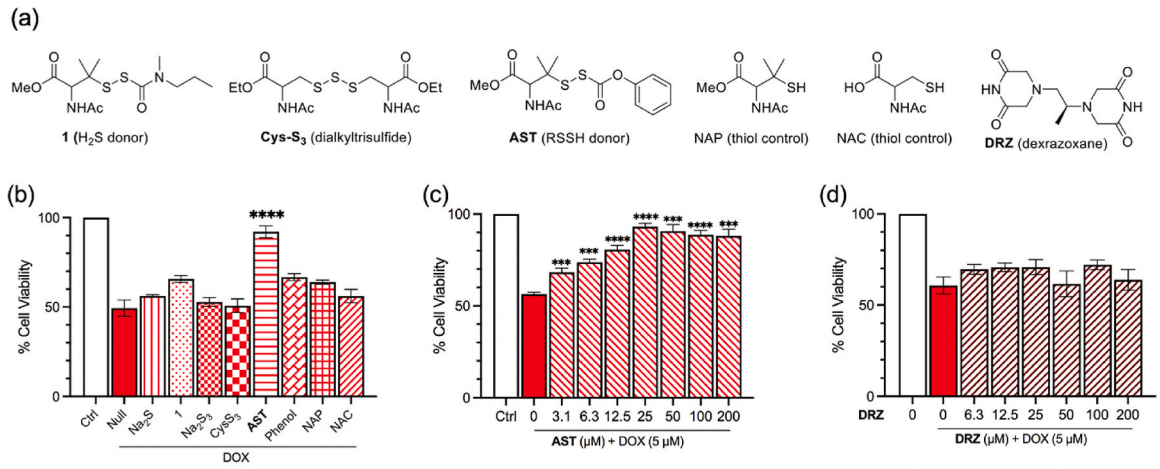

Fig. 1. Cytoprotection by exogenous H_2S, other RSS, and dexrazoxane against DOX-induced toxicity. (a) chemical structures of the RSS and dexrazoxane used in this study. (b) Cell viability of H9c2 cardiac myoblasts pretreated with 25 μM of each RSS for 4 h followed by DOX (5 μM) exposure for 24 h. (c) Dose-dependent protection by RSSH donor **AST** against DOX (5 μM). (d) Dose-dependent protection by dexrazoxane (DRZ) against DOX (5 μM). Cell viability is assessed using CCK-8. Data are shown as the mean ± SEM (n = 4–5 per group). ***P < 0.005 and ****P < 0.001 vs. DOX group.

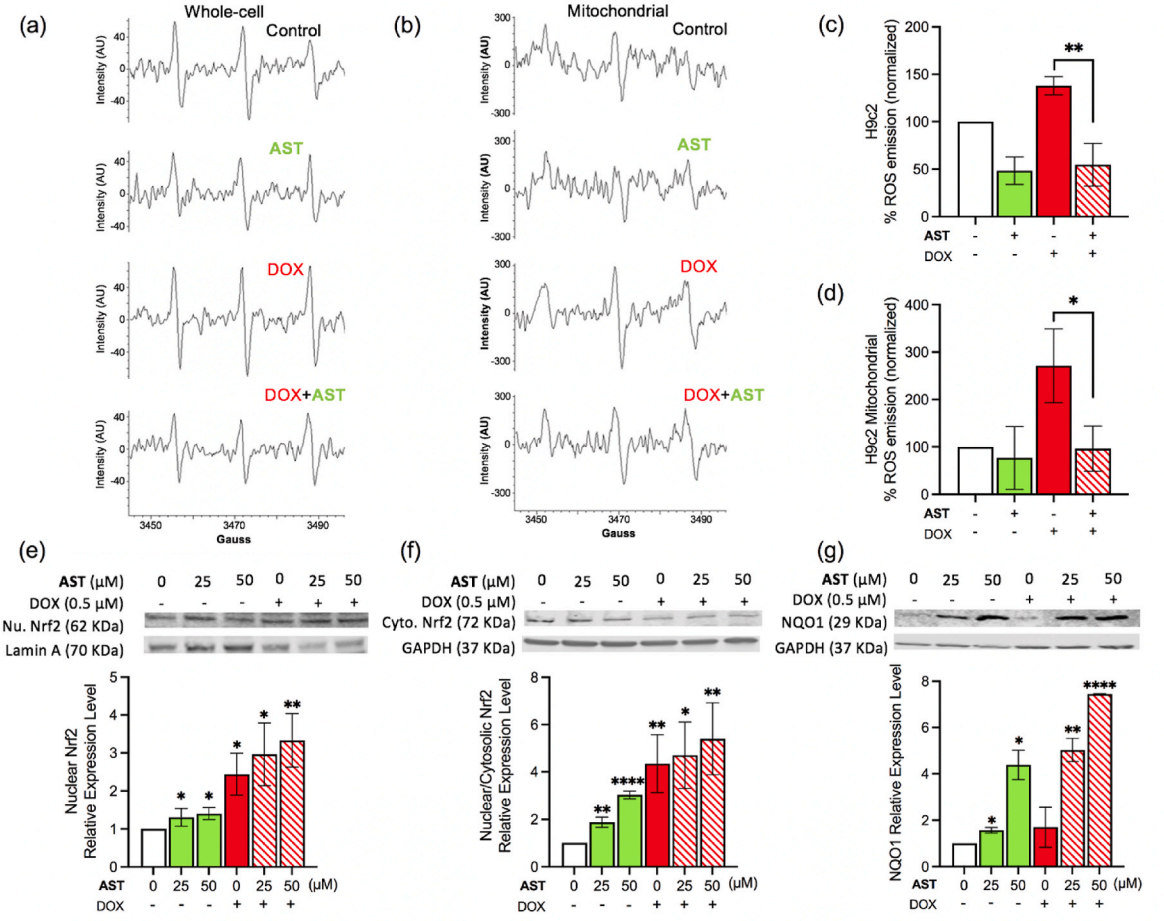

Fig. 2. RSSH donor **AST** reduces DOX-induced ROS levels in H9c2 cardiac myoblasts via activation of Nrf2 and downstream NQO1. Representative EPR spectra showing RSSH-mediated scavenging of (a) whole cell and (b) mitochondrial ROS emission. H9c2 cells were pretreated with **AST** (25 μM) for 4 h followed by treatment with or without DOX (5 μM) for 4 h for whole cell ROS measurement and for 24 h for mitochondrial ROS measurement. (c) Whole-cell, and (d) mitochondrial ROS emission measured by EPR spectroscopy. The relative expression level of (e) nuclear Nrf2; (f) cytosolic Nrf2; and (g) whole cell NQO1 in H9c2 cells. Cells were pretreated with 0, 25, and 50 μM **AST** for 24 h, followed by treatment with either vehicle or 0.5 μM DOX for 24 h. Expression levels of these proteins were measured by immunoblotting. Data are shown as the mean ± SEM (n = 3 per group (e–g) and n = 4 per group (a–d)). *P < 0.05, **P < 0.01 and ****P < 0.001 between respective groups.

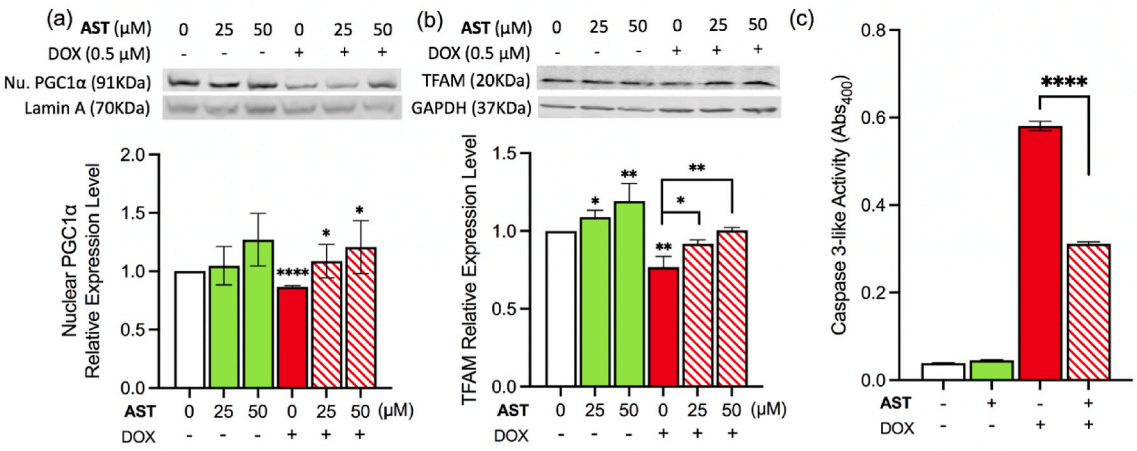

Fig. 3. RSSH donor **AST** restores DOX-mediated decreases in expression of nuclear PGC-1α and its downstream product, cytosolic TFAM. (a) Relative expression level of nuclear PGC-1α, and (b) cytosolic TFAM of H9c2 cells. H9c2 cells were pretreated with 0, 25, and 50 μM **AST** for 24 h followed by treatment with vehicle or 0.5 μM DOX 24 h. Protein expression levels were determined by immunoblotting. (c) Caspase 3-like activity of H9c2 measured using a colorimetric assay. Data are shown as the mean ± SEM (n = 3–4 per group). *P < 0.05, **P < 0.01 and ****P < 0.001 vs. control groups and between respective groups.

Dunn's multiple comparisons test. P values < 0.05 were considered to be statistically significant.

3. Results

3.1. Hydropersulfides outweigh other reactive sulfur species and dexrazoxane in limiting doxorubicin-induced toxicity in H9c2 cells

First, we set out to compare the efficacy of various RSS (Fig. 1a) with H_2S in attenuating/preventing DOX-induced stress in H9c2 cardiomyoblasts. In keeping with previous reports [51,52], H9c2 cells exposed to DOX at 5 μM for 24 h induced significant cytotoxicity (Fig. 1b), analyzed by a CCK-8 assay [39]. The CCK-8 assay utilizes a water-soluble tetrazolium dye WST-8 and measures the reductive capacity of the cell based on the levels and/or availability of intracellular reduced nicotinamides (NADH or NADPH). In this assay, the extracellular WST-8 is reduced by viable cells to a water-soluble formazan compound, which is directly proportional to the number of living cells and is measured spectrophotometrically by absorbance at 450 nm [41]. Also consistent with previous studies [53,54], pretreatment of H9c2 cells with sodium sulfide (Na_2S) at 25 μM for 4 h shows minor protection against DOX. Na_2S is not an ideal H_2S donor because it rapidly releases H_2S in aqueous solution [55], differing from the likely slow enzymatic generation of H_2S in biological systems. Hence, we tested a previously reported H_2S donor **1** that slowly releases H_2S in the presence of thiols with a half-life of approximately 10 min under our experimental conditions (Fig. 1a) [39]. The cell viability assay shows a slightly improved cytoprotection by H_2S donor **1** over Na_2S, consistent with a more significant benefit from slower H_2S donation. Polysulfide species, including inorganic polysulfides and dialkyl polysulfides, have been reported to exert protective effects against oxidative damage [56,57]. Hence, we also measured the cytoprotective potential of polysulfides. Sodium trisulfide (Na_2S_3) and *N*-acetyl-*O*-ethyl cysteine trisulfide (Cys-S_3) are found to be ineffective against DOX toxicity. We then tested RSSH donor **AST** that slowly ($t_{1/2}$ = 129 min) releases *N*-acetylpenicillamine hydropersulfide (NAP-SSH) and phenol as a byproduct [40]. Interestingly, **AST** significantly ameliorates DOX-induced cytotoxicity. Under similar conditions, the phenol byproduct shows only mild protection. Similarly, *N*-acetyl penicillamine (**NAP**), a thiol control that lacks the sulfane sulfur of NAP-SSH also shows mild protection, indicating that **AST** cytoprotective assets stem from RSSH generation. Although both $CysS_3$ and **AST** produce RSSH, the better cytoprotection observed with **AST** is presumably attributed to its ability to generate a *t*-alkyl hydropersulfide, which is more persistent than the primary alkyl hydropersulfide generated from $CysS_3$ [58]. For comparison with a more traditional antioxidant and cytoprotectant, *N*-acetyl cysteine (**NAC**) [59,60], shows only mild protection against DOX under our experimental conditions. The cytoprotective effect of **AST** was independently evaluated using the Sytox Green assay, due to the possibility of background reduction of WST-8 by reactive sulfur species leading to artifactual viability measurements [61]. This assay measures the cell membrane integrity as Sytox Green does not cross intact membranes, but quickly penetrates compromised membranes characteristic of dead cells [62]. Consistent with the observed CCK-8 assay results, **AST** also shows protective effects against DOX-mediated toxicity in H9c2 cells (Supplementary Information, Fig. S8) by the Sytox Green assay.

We next assessed **AST**-derived RSSH beneficial effects at different concentrations. We observed a dose-dependent impact (Fig. 1c). Notably, **AST** shows protection with doses as little as 3.1 μM and maximum protection at 25 μM. Beyond this concentration, cytoprotection marginally declined. We also measured the cytoprotection ability of DRZ, the only FDA-approved drug available to treat DIC [15,63]. H9c2 cells pretreated with DRZ (6.3–200 μM) show only a modest improvement in cell viability (Fig. 1d). From these studies, RSSH donor **AST** is found to be most efficacious against DOX toxicity in H9c2 cardiomyoblasts, and was therefore examined in further studies.

3.2. Hydropersulfides efficiently mitigate DOX-induced ROS emission via Nrf2 activation

We next interrogated the mechanism(s) of RSSH-mediated cytoprotection. Initially, we examined whether pretreatment with RSSH counters the DOX-induced increase in ROS emission. ROS levels in H9c2 cells were measured by electron paramagnetic resonance (EPR) spectroscopy in a real-time and quantitative manner, employing the spin probe 1-hydroxy-3-methoxycarbonyl-2,2,5,5-tetramethyl-pyrrolidine (CMH) [64]. Mitochondrial ROS was measured using 1-hydroxy-4-[2-(triphenylphosphonio)-acetamido]-2,2,6,6-tetramethylpiperidine (mitoTEMPO-H) [44]. The spin probes CMH and Mito-TEMPO-H used in this study are specific for both superoxide and hydroxyl radicals [65]. These oxygen-based radicals oxidize the spin probes to form the corresponding nitroxide radical, which is detected using EPR spectroscopy [66]. As expected, DOX exposure in H9c2 cells results in a major surge of ROS in both whole cells and mitochondria compared with vehicle control (Fig. 2a and b). On the contrary, **AST**-pretreated cells displayed a marked reduction of DOX-induced ROS levels in whole cells and

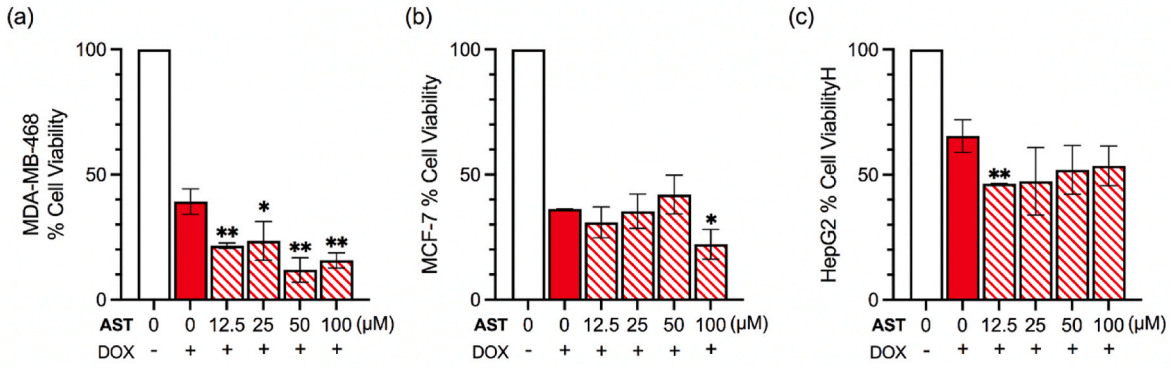

Fig. 4. RSSH donor **AST** increases the efficacy of DOX in cancer cells. Cell viability of (a) MDA-MB-468, (b) MCF-7, and (c) HepG2 cells that were pretreated with **AST** (6.3–100 μM) for 4 h followed by DOX (5 μM) for 24 h. Cell viability is assessed using CCK-8 assay. Data are shown as the mean ± SEM (n = 3 per group). *P < 0.05, and **P < 0.01 vs. DOX group.

mitochondria (Fig. 2c and d). Of note, even without DOX exposure, **AST** treatment significantly decreased ROS levels in whole cells and marginally in mitochondria. Thus, RSSH supplementation effectively mitigates DOX-induced ROS generation in H9c2 cells.

RSS, including RSSH, can activate the Kelch-like ECH-associated protein 1 (Keap1)/transcription nuclear factor erythroid 2-related factor 2 (Nrf2) system [67–69]. The multifunctional regulator Nrf2 is a cytoprotective factor regulating the expression of genes coding for antioxidant, anti-inflammatory, and detoxifying proteins. On these grounds, we tested whether RSSH counter DOX-mediated oxidative stress via Nrf2-dependent antioxidant pathways. Immunoblotting analysis indeed revealed that treatment of H9c2 cells with RSSH donor **AST** at both 25 μM and 50 μM for 24 h modestly increases nuclear Nrf2 levels compared with untreated control (Fig. 2e). Nuclear accumulation of Nrf2 is also demonstrated in cells treated with DOX. Importantly, nuclear Nrf2 levels are found to be markedly elevated when cells are treated with both **AST** and DOX (Fig. 2f). Moreover, the nuclear to the cytosolic ratio of Nrf2 is found to be significantly increased compared to control, confirming the translocation of Nrf2 to the nucleus from the cytosol.

Nrf2 is a critical regulator of intracellular antioxidants and phase II detoxification enzymes by transcriptionally upregulating many antioxidant response element (ARE)-dependent genes [70]. One of the genes regulated through Nrf2 is NAD(P)H quinone oxidoreductase (NQO1), an antioxidant/detoxifying enzyme that scavenges superoxide and protects cells against oxidative stress [71]. **AST** treatment heightens the levels of NQO1 in healthy and DOX-stressed H9c2 cells (Fig. 2g). Hence, these results show that RSSH administration activates Nrf2-dependent pathways, boosting endogenous antioxidant defenses in cardiac cells.

3.3. Hydropersulfides activate PGC-1α and inhibit DOX-induced apoptosis in H9c2 cells

Peroxisome proliferator-activated receptor γ coactivator 1α (PGC-1α) signaling is implicated in mitochondrial biogenesis and is potently activated when cells are exposed to mild oxidative stress to prevent cell damage [72,73]. Hence, we reasoned that PGC-1α could be a good candidate to explain RSSH-imparted benefits. First, using a Western blotting approach, we observed RSSH alone increases PGC-1α protein levels in H9c2 cells (Fig. 3a). Although we anticipated a DOX-mediated increase in PGC-1α expression, a decline was observed instead, presumably due to a large increase in DOX-induced ROS levels beyond the antioxidant capacity of these cells. Interestingly, RSSH pretreatment of H9c2 cells prevented a DOX-induced decrease in PGC-1α levels. PGC-1α interacts with nuclear receptors and transcription factors to further activate the transcription of genes including mitochondrial transcription factor A (TFAM), which is crucial for the transcription and maintenance of mtDNA as well as mtDNA nucleoid formation [74]. Consistent with the reduction of PGC-1α expression, DOX treatment of H9c2 cells shows a decrease in TFAM expression (Fig. 3b). However, **AST** pretreatment moderately rescues the DOX-induced reduction in TFAM expression.

Cardiomyocyte apoptosis is the major feature of DOX cardiotoxicity [75], and inhibiting or attenuating cardiomyocyte apoptosis is an effective strategy to counter DOX-mediated cardiotoxicity [76]. Moreover, PGC-1α-dependent signaling can attenuate ROS-induced apoptotic cell death, for instance, by upregulating Nrf2 [77]. On the heels of this evidence, we then investigated if RSSH could inhibit DOX-induced apoptosis. Several apoptosis markers are known to be upregulated after DOX treatment, for example, caspase 3. We measured caspase-3 activity as a marker of apoptosis in H9c2 cells using a colorimetric assay [45]. Consistent with previous results [78,79], we noted a significant rise in caspase-3 activity in DOX-treated cells (Fig. 3c). Of relevance, **AST** pretreatment protected H9c2 cells from DOX-induced increase of caspase-3 activity, thus suggesting RSSH's ability to mitigate DOX-induced apoptosis. In aggregate, these data sets indicate that RSSH-mediated activation of PGC-1α helps protect against DOX-induced mitochondrial stress, improving biogenesis, and these effects, in turn, better shield cardiomyocytes against DOX-induced apoptosis.

3.4. RSSH potentiate DOX-induced toxicity in cancer cells

A unique challenge in cardio-oncology is minimizing anticancer drugs' cardiac adverse effects without affecting their therapeutic efficacy. Hence, from a translational perspective, we felt it mandatory to determine whether RSSH obliterates or reduces the ability of DOX to inhibit cancer cell proliferative capacity. Intriguingly, pretreating MDA-MB-468 triple-negative breast cancer cells with RSSH donor **AST** exacerbates DOX-induced toxicity at all concentrations examined (6.3–100 μM) (Fig. 4a). Of relevance, **AST** also did not reduce DOX efficacy in two other cancer cell lines, triple-positive breast cancer cells MCF-7 and hepatocellular carcinoma cells HepG2 (Fig. 4b and c). Taken together, this evidence suggests that a) RSSH's effects on DOX efficacy are not limited to one particular cancer cell line and b) at least in the cancer lines examined here, RSSH potentiate DOX antiproliferative properties rather than attenuate them.

3.5. Cancer cells have higher levels of reactive sulfur species and reducing equivalents than cardiac cells

Sulfane sulfur species are enzymatically produced as an adaptive cellular response toward oxidative stress [80,81]. Given this and the above-reported data, we speculate that the RSSH opposing effects observed in cardiac vs. cancer cells could be due to differences in basal (native) RSS levels in cardiac vs. cancer cells. To test this novel possibility, we first measured H_2S levels using HSip-1, a fluorescence probe

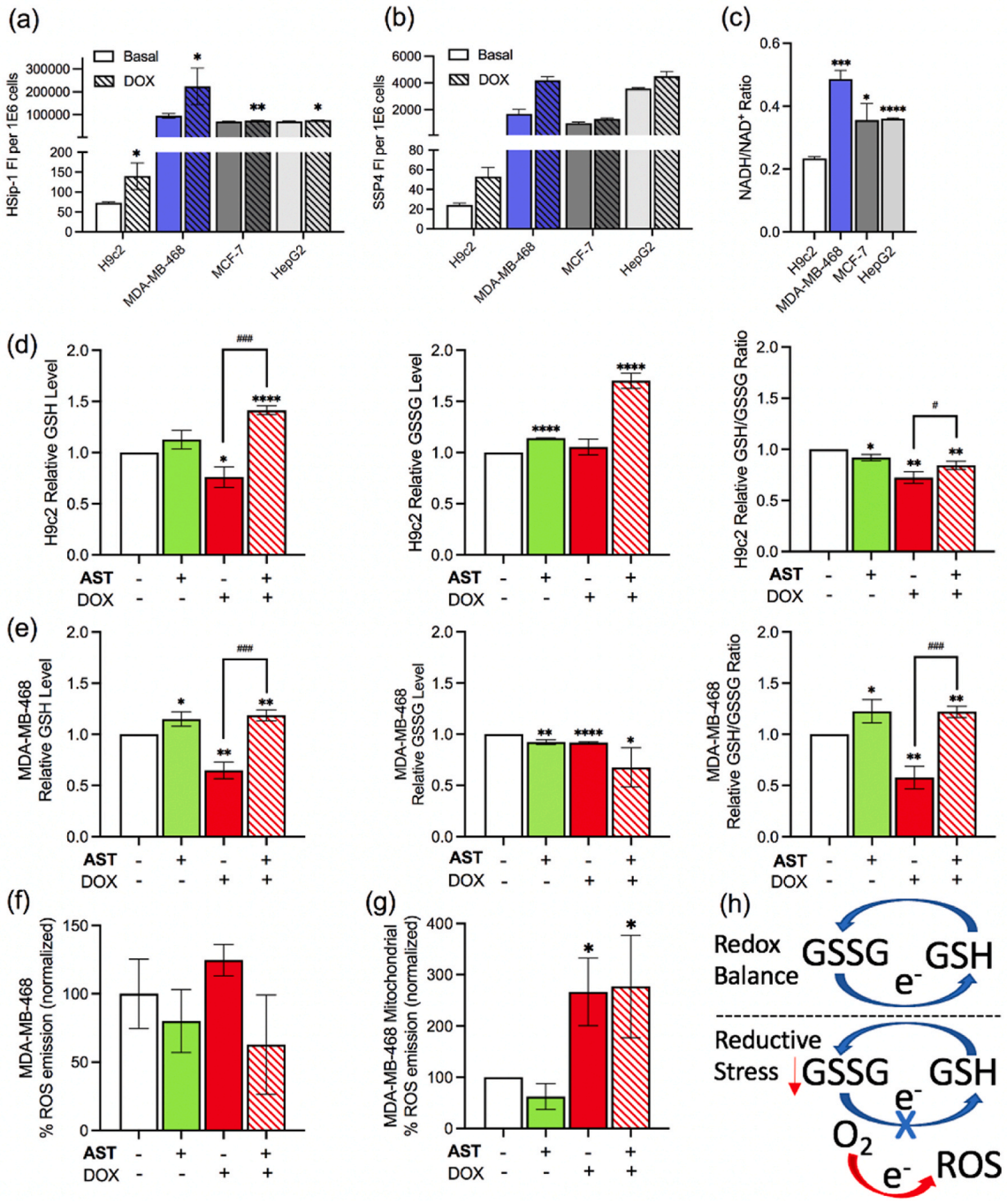

Fig. 5. Cancer cells have higher basal level of H_2S, sulfane sulfur and reducing equivalents. RSSH donor **AST** restores the reduction of GSH in H9c2 cells while depleting GSSG in cancer cells, leading to increased ROS emission in the mitochondria of cancer cells. Basal level of (a) H_2S; (b) sulfane sulfur; and reducing equivalents (c) NADH/NAD^+ of H9c2 and cancer cells. Absolute GSH, absolute GSSG and the GSH/GSSG ratio change of (d) H9c2 and (e) MDA-MB-468 cells. (f) whole cell, and (g) mitochondrial ROS emissions are measured by EPR spectroscopy. (h) Schematic illustration of ROS generation following reductive stress due to lowered mitochondrial GSSG, which normally acts as a primary electron acceptor. Cells were pretreated with 0 or 25 μM **AST** for 4 h followed by co-treatment with 5 μM DOX for 24 h H_2S and sulfane sulfur species levels were measured using fluorescent probes. NADH/NAD^+ and GSH/GSSG ratio were measured using colorimetric assays. Absolute GSH, absolute GSSG, and the GSH/GSSG ratio were measured using colorimetric assays. Data are shown as the mean ± SEM (n = 3 per group (a–e), n = 6–8 per group (f), and n = 6–7 per group (g)). *P < 0.05, **P < 0.01 and ****P < 0.001 vs. control group. #<0.05 and ###<0.005 between respective groups.

that has been extensively used for H_2S detection [48]. Based on the widespread use of HSip-1 for intracellular H_2S detection, we assume that permeability and retention of HSip1 are the same in different cell types. Fluorescence analysis reveals a dramatic difference in levels, with orders of magnitude higher H_2S in cancer cells compared with cardiac cells (Fig. 5a). We then measured sulfane sulfur levels using fluorescence probes SSP4 [47]. Similar to the elevated H_2S levels, we observed significantly higher sulfane sulfur levels in cancer cells compared with H9c2 cells (Fig. 5b). Following established protocols [47,82], we used cetyltrimethylammonium bromide (CTAB) as a surfactant in H_2S and sulfane sulfur detection assays, assuming that at the concentration employed in our study, it does not denature proteins or impact RSS speciation. Importantly, our observation of higher RSS levels in cancer cells is supported by the upregulation of H_2S-producing enzymes in

different cancers, including colon, ovarian, breast, thyroid, prostate, bladder, gastric, hepatoma cancers, etc. [83]. Next, we tested if cells increase H_2S and sulfane sulfur species in response to DOX-induced stress. A rise in H_2S and sulfane sulfur levels were observed in both cardiac and cancer cells after exposure to the DOX (Fig. 5a and b). Thus, both cell types, i.e., cancer and cardiac, enhance the biosynthesis of sulfane sulfur as an adaptive response to protect against DOX-mediated oxidative stress. Elevated RSS levels in cancer cells can be rationalized based on previous findings that stimulation of RSS biosynthesis has been associated with increased cellular proliferation [84].

3.6. RSSH induces reductive stress in DOX-treated cancer cells

Cancer cells possess higher reducing equivalents to counter oxidative stress than normal cells [85]. As a result, we hypothesize that DOX-treated cancer cells may enter a reductive stress state upon supplementation with RSSH. We initially measured basal NADH/NAD^+ ratios to test this hypothesis directly using a colorimetric assay [49]. A significantly higher basal NADH/NAD^+ ratio is observed in MDA-MB-468 cells compared to H9c2 cells (Fig. 5c). Similarly, higher NADH/NAD^+ ratios are observed in MCF-7 and HepG2 cells. Importantly, a higher ratio of GSH/GSSG is also observed in cancer cells compared with the H9c2 cells (Supplementary Information, Fig. S1). These results suggest that cancer cells have higher levels of reducing equivalents such as GSH and NADH compared with cardiac cells, which following DOX treatment presumably makes them susceptible to RSSH-mediated reductive stress. These results also indicate that exogenous augmentation of RSS is likely more deleterious in DOX-treated cancer cells because basal H_2S/sulfane sulfur levels are already very high leading to reductive stress, but protective in DOX-treated cardiac cells where these levels are much lower.

To probe the reductive stress hypothesis further, we measured the change of reducing equivalents following treatment with RSSH donor **AST** and DOX. Treatment of H9c2 cells with DOX decreases both absolute GSH and GSH/GSSG ratios. Still, no significant change in absolute GSSG was observed (Fig. 5d). Interestingly, we found that H9c2 cells pretreated with RSSH are immune to DOX-mediated reduction in GSH levels. Instead, a higher level of GSH and GSSG in the H9c2 cells was detected when treated with both **AST** and DOX (Fig. 5d). These results suggest that RSSH increases GSH levels, and primes cardiac cells to counter DOX-mediated lethal effects. The latter evidence is consistent with our finding that RSSH activates the Nrf2 pathway, which is known to activate GSH biosynthesis [86]. Similarly, for MDA-MB-468 cells, DOX treatment lowers both absolute GSH and GSH/GSGG ratio significantly (Fig. 5e). However, co-treatment of DOX with **AST** results in significantly higher GSH and GSH/GSSG levels, but lower GSSG, than DOX control.

GSSG can serve as an electron acceptor for redox-balancing enzymes in mitochondria [87]. The depletion of GSSG as a result of reductive stress directs electrons to oxygen, resulting in a counter-intuitive burst of mitochondrial ROS species under these conditions(Fig. 5h) [86]. To determine if RSSH treatment indeed results in a surge of mitochondrial ROS levels in cancer cells, we directly measured whole-cell and mitochondrial ROS levels using EPR studies. As expected, treatment of MDA-MB-468 cells with DOX increased ROS levels in both whole cells and mitochondria (Fig. 5f and g and Supplementary Information, Fig. S2). RSSH donor **AST** attenuates DOX-mediated whole-cell ROS levels, but notably exacerbates mitochondrial ROS levels (Fig. 5g). Conversely, RSSH curtails both whole-cell and mitochondrial ROS levels in cardiac cells (Fig. 2a–d). Thus, RSSH instills a reductive stress status in DOX-treated cancer cells, reducing their survival, an effect stemming from their already elevated basal levels of sulfane sulfur and other reducing equivalents.

4. Discussion

Cardio-oncology currently faces at least two primary unmet or partially met clinical milestones: reducing the cardiotoxicity of anticancer drugs, such as anthracyclines including DOX, and not depotentiating their therapeutic efficacy when anthracyclines are combined with cardioprotective agents. Here, we report the following new evidence: 1) RSSH effectively protect H9c2 cardiac cells against DOX-induced toxicity; 2) RSSH supplementation alleviates the DOX-evoked ROS increase in these cells via Nrf2 signaling, boosting antioxidant defenses; 3) RSSH activates PGC-1α, and decrease cardiac cell apoptosis by countering caspase-3 activity; 4) RSSH potentiates anticancer DOX effects in three different cancer cell lines, prompting reductive stress in these cells.

4.1. RSSH are better cardioprotectants than other H_2S-related species due to their distinct chemical properties, i.e., stronger nucleophilic and reducing ability

RSS play a critical role in maintaining redox homeostasis and cell survival via scavenging deleterious ROS and electrophiles [36,80]. However, it is not fully clear if there are any pharmacological advantages in the use of one specific RSS over others. The instability of RSSH species and the rapid interconversion among different RSS further complicates a comparison of their therapeutic effects [33,88]. Building on our previous studies [38–40,89] and searching for novel anti-AIC strategies, we explored RSS such as H_2S, RSSH, inorganic polysulfides, and dialkyl trisulfides as cytoprotective agents against DOX toxicity. To do so, we leveraged small molecule donors that efficiently produce each of the RSS cleanly and examined their individual protective effects against DOX toxicity. Consistent with previous reports [23,24,51,53,54], we observe that Na_2S protects cardiac cells against DOX toxicity. Slower H_2S donor **1** shows slightly improved protection over Na_2S, but polysulfides did not afford protection, at least under our experimental conditions. Similarly, NAC shows mild protection. Interestingly, RSSH donor **AST** exhibits potent cytoprotection superior to FDA-approved DRZ at all concentrations tested. These results are consistent with our recent report demonstrating that RSSH effectively limits irreversible myocardial ischemia-reperfusion injury compared with H_2S and dialkylpolysulfides in the *ex vivo* Langendorff model [38].

Possible explanations for RSSH being a better cytoprotectant than other RSS include their distinct chemical properties, i.e., stronger nucleophilic and reducing ability [36,90,91]. RSSH are among the best H-atom donors identified, reacting with various radicals with rate constants several orders of magnitude greater than those measured for the corresponding RSH [92]. Accordingly, RSSH can potently inhibit ROS-mediated lipid peroxidation and cell membrane damage, potently inhibiting ferroptosis induced in mouse embryonic fibroblasts [80,93]. In addition to the direct scavenging of free radicals, the potency of RSSH may stem from their ability to activate endogenous antioxidant pathways, for example, via Nrf2. Our results clearly demonstrate the RSSH-mediated activation of Nrf2 levels and subsequent activation of antioxidant response element (ARE)-dependent genes as confirmed by elevated levels of NQO1, both in healthy and DOX-stressed H9c2 cells. In addition, our experiments show that **AST** treatment increases PGC-1α levels in H9c2 cells. Thus, RSSH may be uniquely effective as it elicits multifaceted protection modes against DOX toxicity.

4.2. RSSH potentiate rather than diminish DOX anticancer effects

Another intriguing observation is that RSSH pretreatment potentiates, rather than diminishes, DOX's anticancer effects. We attribute this favorable effect to differences in basal and DOX-stressed RSS levels in cardiac vs. cancer cells. The observed rise in H_2S/sulfane sulfur levels after DOX suggests an adaptive response by both cell types. Our finding is consistent with a recent study by Dick and co-workers, who found

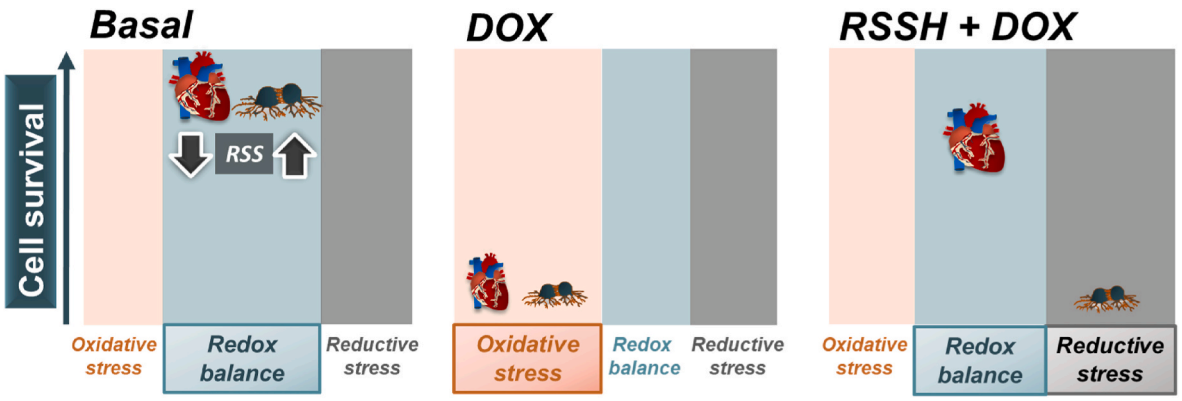

Fig. 6. Schematic representation of the opposing effects of RSSH in cancer cells vs. cardiac cells. Cancer cells have significantly higher levels of basal RSS compared with cardiac cells, with both cells within the redox buffering capacity. DOX treatment induces oxidative stress in both cell types, ultimately leading to cell death. RSSH administration alleviates DOX-induced oxidative stress in cardiac cells, but induces reductive stress in cancer cells that already have higher levels of RSS.

increased RSSH levels in cells after treatment with ferroptosis inducers [80]. In cancer cells, increased ROS production and oxidative stress are instigated by metabolic reprogramming of the rapidly proliferating cells [94]. Our finding supports the idea that cancer cells produce higher levels of RSS to counter the damaging effects of ROS and maintain redox homeostasis. DOX disturbs the redox homeostasis in both cancer and cardiac cells by increasing ROS levels beyond the cellular antioxidant capacity, ultimately leading to cell death. Because cardiac cells have much lower levels of antioxidant enzymes [10] and RSS, exogenous augmentation of RSS via RSSH administration protects cardiac cells against DOX-mediated oxidative stress. On the other hand, since cancer cells have higher basal levels of RSS, administration of RSSH may push cancer cells away from redox balance towards reductive stress, ultimately leading to cell death. However, **AST** treatment alone does not show cytotoxicity against three different cancer cell lines, at least up to 200 μM (Supplementary Information, Fig. S3). These results suggest that DOX-treated cancer cells are sensitive to RSSH-mediated reductive stress (Fig. 6). In aggregate, RSSH precursor **AST** is effective against DOX-induced cardiotoxicity in cardiac cells while maintaining or even enhancing DOX efficacy in killing cancer cells via reductive stress.

In general, the persulfidation of cysteine residues has been proposed as protective by preventing irreversible thiol oxidative and electrophilic damage [30,32,37]. However, it is possible that RSSH can induce oxidative stress via the conversion of protein thiols (PSH) to PSSH or PSSR [81]. Conversion to PSSH and/or PSSR may result in protein inactivation if a particular cysteine residue is crucial to protein activity. Thus, an alternate explanation is that RSSH-mediated oxidative stress results in cancer cells being more vulnerable to DOX toxic effects. Although further work will be necessary to fully understand the opposing action of RSSH in cancer vs. cardiac cells, the data presented here support the use of RSSH donors as a potential treatment for DIC.

Author contributions

Conceptualization, B.M.P., V.S.K., N.P. and J.P.T.; synthesis of RSS donors, V.S.K.; data collection, B.M.P, K.Z., G.K., and C.M.; resources, J.P.T. and N.P.; writing—original draft preparation, V.S.K. and K.Z.; writing—review and editing, V.S.K., K.Z., G.K., C.M., J.P.T., and N.P. All authors have read and agreed to the published version of the manuscript.

Declaration of competing interest

The authors declare that they have no known competing financial interests or personal relationships that could have appeared to influence the work reported in this paper.

Data availability

Data will be made available on request.

Acknowledgments

We gratefully acknowledge the National Institutes of Health (R01 GM145940 to J.P.T. and N.P, T32 GM080189 for support of B.M.P., T32 AG058527 and funds from the Johns Hopkins University Older Americans Independence Center of the National Institute on Aging (under award number P30AG021334) for support of G.K., and R01 HL136918 to N.P.).

Appendix A. Supplementary data

Supplementary data to this article can be found online at https://doi.org/10.1016/j.redox.2023.102625.

Abbreviations

DOX	doxorubicin
DRZ	dexrazoxane
EPR	electron paramagnetic resonance
NAC	*N*-acetylcysteine
NAP	*N*-acetylpenicillamine
Nrf2	Nuclear factor erythroid 2-related factor 2
NQO1	NAD(P)H Quinone Dehydrogenase 1
PGC1α	Peroxisome proliferator-activated receptor γ coactivator 1 α
ROS	reactive oxygen species
TFAM	mitochondrial transcription factor A

References

[1] K.D. Miller, L. Nogueira, T. Devasia, A.B. Mariotto, K.R. Yabroff, A. Jemal, J. Kramer, R.L. Siegel, Cancer treatment and survivorship statistics, 2022, CA Cancer J. Clin. 72 (5) (2022) 409–436.
[2] G.N. Hortobágyi, Anthracyclines in the treatment of cancer, Drugs 54 (4) (1997) 1–7.
[3] E.T.H. Yeh, C.L. Bickford, Cardiovascular complications of cancer therapy: incidence, pathogenesis, diagnosis, and management, J. Am. Coll. Cardiol. 53 (24) (2009) 2231–2247.
[4] P.K. Singal, N. Iliskovic, Doxorubicin-induced cardiomyopathy, N. Engl. J. Med. 339 (13) (1998) 900–905.
[5] S.M. Swain, F.S. Whaley, M.S. Ewer, Congestive heart failure in patients treated with doxorubicin: a retrospective analysis of three trials, Cancer 97 (11) (2003) 2869–2879.
[6] G. Minotti, P. Menna, E. Salvatorelli, G. Cairo, L. Gianni, Anthracyclines: molecular advances and pharmacologic developments in antitumor activity and cardiotoxicity, Pharmacol. Rev. 56 (2) (2004) 185–229.
[7] E. Gammella, F. Maccarinelli, P. Buratti, S. Recalcati, G. Cairo, The role of iron in anthracycline cardiotoxicity, Front. Pharmacol. 5 (25) (2014).

[8] Y. Ichikawa, M. Ghanefar, M. Bayeva, R. Wu, A. Khechaduri, S.V.N. Prasad, R. K. Mutharasan, T.J. Naik, H. Ardehali, Cardiotoxicity of doxorubicin is mediated through mitochondrial iron accumulation, J. Clin. Invest. 124 (2) (2014) 617–630.

[9] S. Zhang, X. Liu, T. Bawa-Khalfe, L.-S. Lu, Y.L. Lyu, L.F. Liu, E.T.H. Yeh, Identification of the molecular basis of doxorubicin-induced cardiotoxicity, Nat. Med. 18 (11) (2012) 1639–1642.

[10] D. Moris, M. Spartalis, E. Tzatzaki, E. Spartalis, G.-S. Karachaliou, A. S. Triantafyllis, G.I. Karaolanis, D.I. Tsilimigras, S. Theocharis, The role of reactive oxygen species in myocardial redox signaling and regulation, Ann. Transl. Med. 5 (16) (2017) 6.

[11] R. D'Oria, R. Schipani, A. Leonardini, A. Natalicchio, S. Perrini, A. Cignarelli, L. Laviola, F. Giorgino, The role of oxidative stress in cardiac disease: from physiological response to injury factor, Oxid. Med. Cell. Longev. 2020 (2020), 5732956.

[12] B.B. Wu, K.T. Leung, E.N. Poon, Mitochondrial-targeted therapy for doxorubicin-induced cardiotoxicity, Int. J. Mol. Sci. 23 (3) (2022) 1912.

[13] K.B. Wallace, V.A. Sardão, P.J. Oliveira, Mitochondrial determinants of doxorubicin-induced cardiomyopathy, Circ. Res. 126 (7) (2020) 926–941.

[14] D.T. Vincent, Y.F. Ibrahim, M.G. Espey, Y.J. Suzuki, The role of antioxidants in the era of cardio-oncology, Cancer Chemother. Pharmacol. 72 (6) (2013) 1157–1168.

[15] R.S. Cvetković, L.J. Scott, Dexrazoxane : a review of its use for cardioprotection during anthracycline chemotherapy, Drugs 65 (7) (2005) 1005–1024.

[16] G.F. Vile, C.C. Winterbourn, N. dl-N N'-dicarboxamidomethyl-, N'-dicarboxymethyl-1,2-diaminopropane (ICRF-198) and d-1,2-bis(3,5-dioxopiperazine-1-yl)propane (ICRF-187) inhibition of Fe3+ reduction, lipid peroxidation, and CaATPase inactivation in heart microsomes exposed to adriamycin, Cancer Res. 50 (8) (1990) 2307–2310.

[17] S.W. Langer, Dexrazoxane for the treatment of chemotherapy-related side effects, Cancer Manag. Res. 6 (2014) 357–363.

[18] C.L. Vogel, E. Gorowski, E. Davila, M. Eisenberger, J. Kosinski, R.P. Agarwal, N. Savaraj, Phase I clinical trial and pharmacokinetics of weekly ICRF-187 (NSC 169780) infusion in patients with solid tumors, Invest. New Drugs 5 (2) (1987) 187–198.

[19] Z. Li, D.J. Polhemus, D.J. Lefer, Evolution of hydrogen sulfide therapeutics to treat cardiovascular disease, Circ. Res. 123 (5) (2018) 590–600.

[20] G.K. Kolluru, X. Shen, C.G. Kevil, Reactive sulfur species, Arterioscler. Thromb. Vasc. Biol. 40 (4) (2020) 874–884.

[21] D.J. Polhemus, K. Kondo, S. Bhushan, S.C. Bir, C.G. Kevil, T. Murohara, D.J. Lefer, J.W. Calvert, Hydrogen sulfide attenuates cardiac dysfunction after heart failure via induction of angiogenesis, Circ. Heart Fail. 6 (5) (2013) 1077–1086.

[22] J.L. Wallace, R. Wang, Hydrogen sulfide-based therapeutics: exploiting a unique but ubiquitous gasotransmitter, Nat. Rev. Drug Discov. 14 (5) (2015) 329–345.

[23] S. Du, Y. Huang, H. Jin, T. Wang, Protective mechanism of hydrogen sulfide against chemotherapy-induced cardiotoxicity, Front. Pharmacol. 9 (32) (2018).

[24] X.-Y. Wang, C.-T. Yang, D.-D. Zheng, L.-Q. Mo, A.-P. Lan, Z.-L. Yang, F. Hu, P.-X. Chen, X.-X. Liao, J.-Q. Feng, Hydrogen sulfide protects H9c2 cells against doxorubicin-induced cardiotoxicity through inhibition of endoplasmic reticulum stress, Mol. Cell. Biochem. 363 (1) (2012) 419–426.

[25] L. Nie, M. Liu, J. Chen, Q. Wu, Y. Li, J. Yi, X. Zheng, J. Zhang, C. Chu, J. Yang, Hydrogen sulfide ameliorates doxorubicin-induced myocardial fibrosis in rats via the PI3K/AKT/mTOR pathway, Mol. Med. Rep. 23 (4) (2021) 299.

[26] Q. Hu, R.D. Yammani, H. Brown-Harding, D.R. Soto-Pantoja, L.B. Poole, J. C. Lukesh, Mitigation of doxorubicin-induced cardiotoxicity with an H2O2-Activated, H2S-Donating hybrid prodrug, Redox Biol. 53 (2022), 102338.

[27] M.R. Filipovic, J. Zivanovic, B. Alvarez, R. Banerjee, Chemical biology of H2S signaling through persulfidation, Chem. Rev. 118 (3) (2018) 1253–1337.

[28] C. Gotor, A. Aroca, L.C. Romero, Persulfidation is the mechanism underlying sulfide-signaling of autophagy, Autophagy 18 (3) (2022) 695–697.

[29] B. Murphy, R. Bhattacharya, P. Mukherjee, Hydrogen sulfide signaling in mitochondria and disease, FASEB J. 33 (12) (2019) 13098–13125.

[30] J.M. Fukuto, J. Lin, V.S. Khodade, J.P. Toscano, Predicting the possible physiological/biological utility of the hydropersulfide functional group based on its chemistry: similarities between hydropersulfides and selenols, Antioxid. Redox Signal 33 (18) (2020) 1295–1307.

[31] Y. Shinkai, Y. Kumagai, Sulfane sulfur in toxicology: a novel defense system against electrophilic stress, Toxicol. Sci. 170 (1) (2019) 3–9.

[32] J.M. Fukuto, L.J. Ignarro, P. Nagy, D.A. Wink, C.G. Kevil, M. Feelisch, M. M. Cortese-Krott, C.L. Bianco, Y. Kumagai, A.J. Hobbs, J. Lin, T. Ida, T. Akaike, Biological hydropersulfides and related polysulfides – a new concept and perspective in redox biology, FEBS Lett. 592 (12) (2018) 2140–2152.

[33] V.S. Khodade, S.C. Aggarwal, A. Eremiev, E. Bao, S. Porche, J.P. Toscano, Development of hydropersulfide donors to study their chemical biology, Antioxid. Redox Signal. 36 (4–6) (2022) 309–326.

[34] T. Ida, T. Sawa, H. Ihara, Y. Tsuchiya, Y. Watanabe, Y. Kumagai, M. Suematsu, H. Motohashi, S. Fujii, T. Matsunaga, M. Yamamoto, K. Ono, N.O. Devarie-Baez, M. Xian, J.M. Fukuto, T. Akaike, Reactive cysteine persulfides and S-polythiolation regulate oxidative stress and redox signaling, Proc. Natl. Acad. Sci. USA 111 (21) (2014) 7606–7611.

[35] M. Iciek, A. Bilska-Wilkosz, M. Kozdrowicki, M. Górny, Reactive sulfur species and their significance in health and disease, Biosci. Rep. 42 (9) (2022).

[36] J.M. Fukuto, A.J. Hobbs, A comparison of the chemical biology of hydropersulfides (RSSH) with other protective biological antioxidants and nucleophiles, Nitric Oxide 107 (2021) 46–57.

[37] J.M. Fukuto, The biological/physiological utility of hydropersulfides (RSSH) and related species: what is old is new again, Antioxid. Redox Signal. 36 (4–6) (2022) 244–255.

[38] B.M. Pharoah, V.S. Khodade, A. Eremiev, E. Bao, T. Liu, B. O'Rourke, N. Paolocci, J.P. Toscano, Hydropersulfides (RSSH) outperform post-conditioning and other reactive sulfur species in limiting ischemia–reperfusion injury in the isolated mouse heart, Antioxidants 11 (5) (2022) 1010.

[39] V.S. Khodade, B.M. Pharoah, N. Paolocci, J.P. Toscano, Alkylamine-substituted perthiocarbamates: dual precursors to hydropersulfide and carbonyl sulfide with cardioprotective actions, J. Am. Chem. Soc. 142 (9) (2020) 4309–4316.

[40] V.S. Khodade, S.C. Aggarwal, B.M. Pharoah, N. Paolocci, J.P. Toscano, Alkylsulfenyl thiocarbonates: precursors to hydropersulfides potently attenuate oxidative stress, Chem. Sci. 12 (23) (2021) 8252–8259.

[41] M. Ishiyama, Y. Miyazono, K. Sasamoto, Y. Ohkura, K. Ueno, A highly water-soluble disulfonated tetrazolium salt as a chromogenic indicator for NADH as well as cell viability, Talanta 44 (7) (1997) 1299–1305.

[42] S.P. Chelko, G. Keceli, A. Carpi, N. Doti, J. Agrimi, A. Asimaki, C.B. Beti, M. Miyamoto, N. Amat-Codina, D. Bedja, A.-C. Wei, B. Murray, C. Tichnell, C. Kwon, H. Calkins, C.A. James, B. O'Rourke, M.K. Halushka, E. Melloni, J. E. Saffitz, D.P. Judge, M. Ruvo, R.N. Kitsis, P. Andersen, F. Di Lisa, N. Paolocci, Exercise triggers CAPN1-mediated AIF truncation, inducing myocyte cell death in arrhythmogenic cardiomyopathy, Sci. Transl. Med. 13 (581) (2021), eabf0891.

[43] G. Keceli, A. Gupta, J. Sourdon, R. Gabr, M. Schär, S. Dey, C.G. Tocchetti, A. Stuber, J. Agrimi, Y. Zhang, M. Leppo, C. Steenbergen, S. Lai, L.R. Yanek, B. O'Rourke, G. Gerstenblith, P.A. Bottomley, Y. Wang, N. Paolocci, R.G. Weiss, Mitochondrial creatine kinase attenuates pathologic remodeling in heart failure, Circ. Res. 130 (5) (2022) 741–759.

[44] S. Scheinok, T. Capeloa, P.E. Porporato, P. Sonveaux, B. Gallez, An EPR study using cyclic hydroxylamines to assess the level of mitochondrial ROS in superinvasive cancer cells, Cell Biochem. Biophys. 78 (3) (2020) 249–254.

[45] J.-S. Kwon, S.M. Schumacher, E. Gao, J.K. Chuprun, J. Ibetti, R. Roy, M. Khan, R. Kishore, W.J. Koch, Characterization of βARKct engineered cellular extracellular vesicles and model specific cardioprotection, Am. J. Physiol. Heart Circ. Physiol. 320 (4) (2021) H1276–H1289.

[46] U.K. Laemmli, Cleavage of structural proteins during the assembly of the head of bacteriophage T4, Nature 227 (5259) (1970) 680–685.

[47] M. Shieh, X. Ni, S. Xu, S.P. Lindahl, M. Yang, T. Matsunaga, R. Flaumenhaft, T. Akaike, M. Xian, Shining a light on SSP4: a comprehensive analysis and biological applications for the detection of sulfane sulfurs, Redox Biol. 56 (2022), 102433.

[48] K. Sasakura, K. Hanaoka, N. Shibuya, Y. Mikami, Y. Kimura, T. Komatsu, T. Ueno, T. Terai, H. Kimura, T. Nagano, Development of a highly selective fluorescence probe for hydrogen sulfide, J. Am. Chem. Soc. 133 (45) (2011) 18003–18005.

[49] J. Zhu, G. Wu, L. Song, L. Cao, Z. Tan, M. Tang, Z. Li, D. Shi, S. Zhang, J. Li, NKX2-8 deletion-induced reprogramming of fatty acid metabolism confers chemoresistance in epithelial ovarian cancer, EBioMedicine 43 (2019) 238–252.

[50] R. Manzoor, A. Rasool, M. Ahmed, U. Kaleem, L.N. Duru, H. Ma, Y. Deng, Synergistic neuroprotective effect of endogenously-produced hydroxytyrosol and synaptic vesicle proteins on pheochromocytoma cell line against salsolinol, Molecules 25 (7) (2020) 1715.

[51] R. Guo, J. Lin, W. Xu, N. Shen, L. Mo, C. Zhang, J. Feng, Hydrogen sulfide attenuates doxorubicin-induced cardiotoxicity by inhibition of the p38 MAPK pathway in H9c2 cells, Int. J. Mol. Med. 31 (3) (2013) 644–650.

[52] R. Johnson, S. Shabalala, J. Louw, A.P. Kappo, C.J.F. Muller, Aspalathin reverts doxorubicin-induced cardiotoxicity through increased autophagy and decreased expression of p53/mTOR/p62 signaling, Molecules 22 (10) (2017) 1589.

[53] M.H. Liu, Y. Zhang, X.L. Lin, J. He, T.P. Tan, S.J. Wu, S. Yu, L. Chen, Y.D. Chen, H. Y. Fu, C. Yuan, J. Li, Hydrogen sulfide attenuates doxorubicin-induced cardiotoxicity by inhibiting calreticulin expression in H9c2 cells, Mol. Med. Rep. 12 (4) (2015) 5197–5202.

[54] M.-H. Liu, Y. Zhang, J. He, T.-P. Tan, S.-J. Wu, D.-M. Guo, H. He, J. Peng, Z.-H. Tang, Z.-S. Jiang, Hydrogen sulfide protects H9c2 cardiac cells against doxorubicin-induced cytotoxicity through the PI3K/Akt/FoxO3a pathway, Int. J. Mol. Med. 37 (6) (2016) 1661–1668.

[55] E. Magli, E. Perissutti, V. Santagada, G. Caliendo, A. Corvino, G. Esposito, G. Esposito, F. Fiorino, M. Migliaccio, A. Scognamiglio, B. Severino, R. Sparaco, F. Frecentese, H2S donors and their use in medicinal chemistry, Biomolecules 11 (12) (2021) 1899.

[56] H. Kimura, Signaling molecules: hydrogen sulfide and polysulfide, Antioxid. Redox Signal. 22 (5) (2015) 362–376.

[57] T. Zhang, K. Ono, H. Tsutsuki, H. Ihara, W. Islam, T. Akaike, T. Sawa, Enhanced cellular polysulfides negatively regulate TLR4 signaling and mitigate lethal endotoxin shock, Cell Chem. Biol. 26 (5) (2019) 686–698.e4.

[58] K.G. Fosnacht, M.M. Cerda, E.J. Mullen, H.C. Pigg, M.D. Pluth, Esterase-activated perthiocarbonate persulfide donors provide insights into persulfide persistence and stability, ACS Chem. Biol. 17 (2) (2022) 331–339.

[59] D. Ezeriņa, Y. Takano, K. Hanaoka, Y. Urano, T.P. Dick, N-acetyl cysteine functions as a fast-acting antioxidant by triggering intracellular H2S and sulfane sulfur production, Cell Chem. Biol. 25 (4) (2018) 447–459.e4.

[60] V. Arica, H. Demir İ, M. Tutanc, F. Basarslan, S. Arica, M. Karcoıglu, H. Öztürk, A. Nacar, N-acetylcysteine prevents doxorubucine-induced cardiotoxicity in rats, Hum. Exp. Toxicol. 32 (6) (2013) 655–661.

[61] C.L. Bianco, T. Akaike, T. Ida, P. Nagy, V. Bogdandi, J.P. Toscano, Y. Kumagai, C. F. Henderson, R.N. Goddu, J. Lin, J.M. Fukuto, The reaction of hydrogen sulfide with disulfides: formation of a stable trisulfide and implications for biological systems, Br. J. Pharmacol. 176 (4) (2019) 671–683.

[62] L.J. Jones, V.L. Singer, Fluorescence microplate-based assay for tumor necrosis factor activity using SYTOX green stain, Anal. Biochem. 293 (1) (2001) 8–15.

[63] A.V.S. Macedo, L.A. Hajjar, A.R. Lyon, B.R. Nascimento, A. Putzu, L. Rossi, R. B. Costa, G. Landoni, A. Nogueira-Rodrigues, A.L.P. Ribeiro, Efficacy of dexrazoxane in preventing anthracycline cardiotoxicity in breast cancer, JACC CardioOncol. 1 (1) (2019) 68–79.
[64] S.I. Dikalov, I.A. Kirilyuk, M. Voinov, I.A. Grigor'ev, EPR detection of cellular and mitochondrial superoxide using cyclic hydroxylamines, Free Radic. Res. 45 (4) (2011) 417–430.
[65] J.P. Gotham, R. Li, T.E. Tipple, J.R. Lancaster Jr., T. Liu, Q. Li, Quantitation of spin probe-detectable oxidants in cells using electron paramagnetic resonance spectroscopy: to probe or to trap? Free Radic. Biol. Med. 154 (2020) 84–94.
[66] K. Abbas, N. Babić, F. Peyrot, Use of spin traps to detect superoxide production in living cells by electron paramagnetic resonance (EPR) spectroscopy, Methods 109 (2016) 31–43.
[67] S. Koike, Y. Ogasawara, N. Shibuya, H. Kimura, K. Ishii, Polysulfide exerts a protective effect against cytotoxicity caused by t-buthylhydroperoxide through Nrf2 signaling in neuroblastoma cells, FEBS Lett. 587 (21) (2013) 3548–3555.
[68] S. Koike, S. Nishimoto, Y. Ogasawara, Cysteine persulfides and polysulfides produced by exchange reactions with H(2)S protect SH-SY5Y cells from methylglyoxal-induced toxicity through Nrf2 activation, Redox Biol. 12 (2017) 530–539.
[69] J.W. Calvert, S. Jha, S. Gundewar, J.W. Elrod, A. Ramachandran, C.B. Pattillo, C. G. Kevil, D.J. Lefer, Hydrogen sulfide mediates cardioprotection through Nrf2 signaling, Circ. Res. 105 (4) (2009) 365–374.
[70] C. Tonelli, I.I.C. Chio, D.A. Tuveson, Transcriptional regulation by Nrf2, Antioxid. Redox Signal 29 (17) (2018) 1727–1745.
[71] A.T. Dinkova-Kostova, P. Talalay, NAD(P)H:quinone acceptor oxidoreductase 1 (NQO1), a multifunctional antioxidant enzyme and exceptionally versatile cytoprotector, Arch. Biochem. Biophys. 501 (1) (2010) 116–123.
[72] K. Aquilano, S. Baldelli, B. Pagliei, S.M. Cannata, G. Rotilio, M.R. Ciriolo, p53 orchestrates the PGC-1α-mediated antioxidant response upon mild redox and metabolic imbalance, Antioxid. Redox Signal. 18 (4) (2013) 386–399.
[73] R. Ventura-Clapier, A. Garnier, V. Veksler, Transcriptional control of mitochondrial biogenesis: the central role of PGC-1α, Cardiovasc. Res. 79 (2) (2008) 208–217.
[74] D. Kang, S.H. Kim, N. Hamasaki, Mitochondrial transcription factor A (TFAM): roles in maintenance of mtDNA and cellular functions, Mitochondrion 7 (1–2) (2007) 39–44.
[75] E. Christidi, L.R. Brunham, Regulated cell death pathways in doxorubicin-induced cardiotoxicity, Cell Death Dis. 12 (4) (2021) 339.
[76] P.S. Rawat, A. Jaiswal, A. Khurana, J.S. Bhatti, U. Navik, Doxorubicin-induced cardiotoxicity: an update on the molecular mechanism and novel therapeutic strategies for effective management, Biomed. Pharmacother. 139 (2021), 111708.
[77] H.-I. Choi, H.-J. Kim, J.-S. Park, I.-J. Kim, E.H. Bae, S.K. Ma, S.W. Kim, PGC-1α attenuates hydrogen peroxide-induced apoptotic cell death by upregulating Nrf-2 via GSK3β inactivation mediated by activated p38 in HK-2 Cells, Sci. Rep. 7 (1) (2017) 4319.
[78] E.A. Konorev, S. Vanamala, B. Kalyanaraman, Differences in doxorubicin-induced apoptotic signaling in adult and immature cardiomyocytes, Free Radic. Biol. Med. 45 (12) (2008) 1723–1728.
[79] A.C. Moreira, A.F. Branco, S.F. Sampaio, T. Cunha-Oliveira, T.R. Martins, J. Holy, P.J. Oliveira, V.A. Sardão, Mitochondrial apoptosis-inducing factor is involved in doxorubicin-induced toxicity on H9c2 cardiomyoblasts, Biochim. Biophys. Acta, Mol. Basis Dis. 1842 (12) (2014) 2468–2478. Part A).
[80] U. Barayeu, D. Schilling, M. Eid, T.N. Xavier da Silva, L. Schlicker, N. Mitreska, C. Zapp, F. Gräter, A.K. Miller, R. Kappl, A. Schulze, J.P. Friedmann Angeli, T. P. Dick, Hydropersulfides inhibit lipid peroxidation and ferroptosis by scavenging radicals, Nat. Chem. Biol. (2022), https://doi.org/10.1038/s41589-022-01145-w.
[81] C.H. Switzer, J.M. Fukuto, The antioxidant and oxidant properties of hydropersulfides (RSSH) and polysulfide species, Redox Biol. 57 (2022), 102486.
[82] N. Takahashi, F.-Y. Wei, S. Watanabe, M. Hirayama, Y. Ohuchi, A. Fujimura, T. Kaitsuka, I. Ishii, T. Sawa, H. Nakayama, T. Akaike, K. Tomizawa, Reactive sulfur species regulate tRNA methylthiolation and contribute to insulin secretion, Nucleic Acids Res. 45 (1) (2017) 435–445.
[83] R.-H. Wang, Y.-H. Chu, K.-T. Lin, The hidden role of hydrogen sulfide metabolism in cancer, Int. J. Mol. Sci. 22 (12) (2021) 6562.
[84] K. Erdélyi, T. Ditrói, H.J. Johansson, Á. Czikora, N. Balog, L. Silwal-Pandit, T. Ida, J. Olasz, D. Hajdú, Z. Mátrai, O. Csuka, K. Uchida, J. Tóvári, O. Engebraten, T. Akaike, A.-L.B. Dale, M. Kásler, J. Lehtiö, P. Nagy, Reprogrammed transsulfuration promotes basal-like breast tumor progression via realigning cellular cysteine persulfidation, Proc. Natl. Acad. Sci. U.S.A. 118 (45) (2021), e2100050118.
[85] Z. Zhelev, I. Aoki, V. Gadjeva, B. Nikolova, R. Bakalova, T. Saga, Tissue redox activity as a sensing platform for imaging of cancer based on nitroxide redox cycle, Eur. J. Cancer 49 (6) (2013) 1467–1478.
[86] G. Shanmugam, M. Narasimhan, S. Tamowski, V. Darley-Usmar, N.S. Rajasekaran, Constitutive activation of Nrf2 induces a stable reductive state in the mouse myocardium, Redox Biol. 12 (2017) 937–945.
[87] P. Korge, G. Calmettes, J.N. Weiss, Increased reactive oxygen species production during reductive stress: the roles of mitochondrial glutathione and thioredoxin reductases, Biochim. Biophys. Acta Bioenerg. 1847 (6) (2015) 514–525.
[88] K.M. Dillon, J.B. Matson, A review of chemical tools for studying small molecule persulfides: detection and delivery, ACS Chem. Biol. 16 (7) (2021) 1128–1141.
[89] V.S. Khodade, J.P. Toscano, Development of S-substituted thioisothioureas as efficient hydropersulfide precursors, J. Am. Chem. Soc. 140 (50) (2018) 17333–17337.
[90] E. Cuevasanta, M.N. Möller, B. Alvarez, Biological chemistry of hydrogen sulfide and persulfides, Arch. Biochem. Biophys. 617 (2017) 9–25.
[91] J. Zarenkiewicz, V.S. Khodade, J.P. Toscano, Reaction of nitroxyl (HNO) with hydrogen sulfide and hydropersulfides, J. Org. Chem. 86 (1) (2021) 868–877.
[92] J.-P.R. Chauvin, M. Griesser, D.A. Pratt, Hydropersulfides: H-atom transfer agents par excellence, J. Am. Chem. Soc. 139 (18) (2017) 6484–6493.
[93] Z. Wu, V.S. Khodade, J.-P.R. Chauvin, D. Rodriguez, J.P. Toscano, D.A. Pratt, Hydropersulfides inhibit lipid peroxidation and protect cells from ferroptosis, J. Am. Chem. Soc. 144 (34) (2022) 15825–15837.
[94] A. Ghoneum, A.Y. Abdulfattah, B.O. Warren, J. Shu, N. Said, Redox homeostasis and metabolism in cancer: a complex mechanism and potential targeted therapeutics, Int. J. Mol. Sci. 21 (9) (2020) 3100.